NJC

Accepted Manuscript

This is an *Accepted Manuscript*, which has been through the Royal Society of Chemistry peer review process and has been accepted for publication.

Accepted Manuscripts are published online shortly after acceptance, before technical editing, formatting and proof reading. Using this free service, authors can make their results available to the community, in citable form, before we publish the edited article. We will replace this *Accepted Manuscript* with the edited and formatted *Advance Article* as soon as it is available.

You can find more information about *Accepted Manuscripts* in the Information for Authors.

Please note that technical editing may introduce minor changes to the text and/or graphics, which may alter content. The journal's standard Terms & Conditions and the Ethical guidelines still apply. In no event shall the Royal Society of Chemistry be held responsible for any errors or omissions in this *Accepted Manuscript* or any consequences arising from the use of any information it contains.

ROYAL SOCIETY OF CHEMISTRY

www.rsc.org/njc

NJC

RSCPublishing

LETTER

Facile hydroxyl-assisted synthesis of morphological Cu_2O architectures and their shape-dependent photocatalytic performances†

Cite this: DOI: 10.1039/c3nj00000x

Received 00th XXXXX 2013,
Accepted 00th XXXXX 2013

DOI: 10.1039/c3nj00000x

www.rsc.org/njc

Linli Tang, Jian Lv, Shaodong Sun, Xiaozhe Zhang, Chuncai Kong, Xiaoping Song and Zhimao Yang*

An interesting morphology-evolution of Cu_2O from cubic, edge-truncated cubic, edge- and corner-truncated octahedral, truncated octahedral, and finally to octahedral architectures were readily achieved by adjusting the concentration of hydroxyl. When evaluated for their photocatalytic performances, these polyhedral Cu_2O crystals manifest shape-dependent properties.

During the past decades, much efforts has been developed to study the controlled synthesis of inorganic micro- and nanostructures with well-defined shapes and sizes, on account of their influences on the chemical, physical, optical and catalytic properties of materials. As an important p-type semiconductor, cuprous oxide (Cu_2O) has attracted extensive attention for potential applications in solar energy conversion,[1] catalysis,[2] gas sensors,[3] negative electrode material for lithium-ion batteries,[4] template,[5] and metal-insulator-metal resistive switching memory.[6] In the past few years, much excellent work has been devoted to tuning the structure of materials on specific morphology owing to their potential applications, which has been one of the important goals of Cu_2O crystals research, thus controlled synthesized of Cu_2O with uniform shapes became an important issue.

Numerous of Cu_2O architectures with well-controlled uniform morphologies have been synthesized, such as nanowires,[7] nanospheres,[8] polyhedra,[9-16] hollow structures,[17] and hierarchical structures.[18,19] Among the morphological Cu_2O, cubic and octahedral geometries are the basic structures, from which the other complex structures can be achieved. Recently, various methods have been reported for the production of Cu_2O with various morphologies. For example, Xue and coworkers have reported that the morphology-evolution of Cu_2O from nanowires to polyhedra by the control of the pH-dependent precursor species $Cu_2(OH)_3NO_3$, $Cu(OH)_2$ and $Cu(OH)_4^{2-}$ in a starch reduction system.[20] Huang and coworkers have obtained the synthesis of Cu_2O crystals from cubic to rhombic dodecahedral structures by adjusting the amounts of $NH_2OH{\cdot}HCl$, whereby the solution pH decreases gradually, the morphologies of Cu_2O can from nanocubes to the edge- and corner-truncated octahedra, all-corner-truncated rhombic dodecahedra, the {100}-truncated rhombic dodecahedra and the rhombic dodecahedra.[21] Yuan and coworkers have achieved Cu_2O with various morphologies from octahedra to hollow structures by simply adjustment the concentration of glucose, reaction temperature and time.[22] Although several morphology-evolution processes have been reported, the morphological connection among cubes, edge-truncated cubes, edge- and corner-truncated octahedra, truncated octahedra and octahedra has been rarely revealed.

Herein, we successfully synthesized Cu_2O crystals with systematic shape-evolution from cubes to edge-truncated cubes, edge- and corner-truncated octahedra, truncated octahedra and octahedra. The growth mechanism of these morphological Cu_2O architectures was investigated in detailed. The shape-dependent photocatalytic performances of the polyhedral Cu_2O crystals were demonstrated.

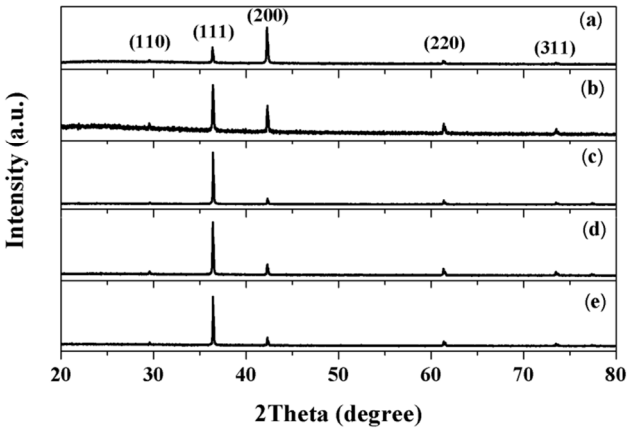

Fig. 1 XRD patterns of the Cu_2O crystals prepared with different morphologies: (a) cubes; (b) edge-truncated cubes; (c) edge- and corner-truncated octahedra; (d) truncated octahedra; (e) octahedra.

The phase structure of the as-prepared products was examined by X-ray diffraction (XRD) characterization. Fig. 1 displays the XRD patterns of as-prepared products with different morphologies. All the diffraction peaks are indexed according to the standard structure of Cu_2O (space group: $Pn\bar{3}m$, lattice constant a = 0.427 nm, JCPDS file

NO. 05-0667). No peaks of impurities such as copper or cupric oxide were detected, suggesting the high purity of the as-obtained products. The strong and sharp peaks indicate that the obtained Cu_2O crystals are highly crystalline. Meanwhile, the diffraction patterns show clearly a transition in the relative intensities of the (111) and the (200) peaks with morphologies change.

The synthesis of Cu_2O crystals with different morphologies can be effectively achieved by a solution phase method. This method is based on the reduction of the Cupric sulfate ($CuSO_4$), Ethylene diamine tetraacetic acid (EDTA), and sodium hydroxide (NaOH) aqueous system with hydroquinone ($C_6H_6O_2$) EDTA serves as chelating reagent, Cu(II)–EDTA complex is prepared in aqueous solution at certain temperature (55°C) from $CuSO_4$ and EDTA, the existence of Cu(II)-EDTA complex can retain the precipitation of Cu(II) cations in the alkaline environment, which can make the Cu_2O participate slowly and homogeneously from the solution during the crystallization process.[23] NaOH is used as a coordination agent to fabricate the complex-precursor, and the characteristics precursor can determine the aggregation of the Cu_2O seeds during the initial growth stages. $C_6H_6O_2$ is a weak multifunctional reducer, which can act both as a reducing agent and as a ligand.[24]

When appropriate amounts of $CuSO_4$, EDTA, NaOH and $C_6H_6O_2$ were added into the solution at certain temperature, Cu_2O can be synthesized from the following reaction. Firstly, Cu(II)-EDTA complex can formed as the precursor. Secondly, hydroxyl (OH^-) ions were added into the Cu(II)-EDTA complex solution, $Cu(OH)_2$ was the first formation from the solution (eqn (1)). When the concentration of OH^- ions was high, $[Cu(OH)_4]^{2-}$ complexes would be formed (eqn (2)). Finally, under the introduction of $C_6H_6O_2$, Cu_2O was synthesized by the $[Cu(OH)_4]^{2-}$ species (eqn (3)).

$$\text{Cu(II)-EDTA} + 2OH^- \rightarrow Cu(OH)_2\downarrow \quad (1)$$

$$Cu(OH)_2 + 2OH^- \rightarrow [Cu(OH)_4]^{2-} \quad (2)$$

$$2[Cu(OH)_4]^{2-} + C_6H_6O_2 \rightarrow Cu_2O\downarrow + C_6H_4O_2 + 4OH^- + 3H_2O \quad (3)$$

On the basic of the above reaction mechanism, it is found that the morphology-evolution of Cu_2O crystals is essentially determined by the $[Cu(OH)_4]^{2-}$ precursors fabricated in different concentrations of OH^- ions. The different concentrations of $[Cu(OH)_4]^{2-}$ can influence the reaction process (eqn (3)), which might affect the competition between the thermodynamics and kinetics during the reaction of precursors, nucleation and growth of Cu_2O crystals.[25]

Here, morphological Cu_2O crystals can be synthesized by simply altering the concentration of OH^- ions. Fig. 2 displayed a series of SEM images of the Cu_2O architectures under the concentrations of OH^- ions from 0.6 M to 6.8 M. It was found that in the absence of OH^- ions, no precipitate was obtained in the reaction system. Fig. 2a showed the SEM image of Cu_2O cubes, when the concentration of OH^- ions was 0.6 M, it can be clearly seen that these particles composed of six {100} planes (Fig. 2a ~ Fig. 2b). As the concentration of OH^- ions increased to 1.6 M, the edge-truncated cubes can be obtained (Fig. 2d ~ Fig. 2e), compared with the Cu_2O cubes, the emerging new facets in the Cu_2O crystal were {110} facets, which grew between any two adjacent {100} facets. As the concentration of OH^- ions elevated to 3.96 M, the edge- and corner-truncated octahedral architecture achieved along with {111} facets (Fig. 2g ~ Fig. 2h). The {111} facets grew among the relatively newer facets {110} of edge-truncated cubes. In other words, edge- and corner-truncated octahedra can be seen as cutting the 8 vertices of the edge-truncated cubes. With the concentration of OH^- ions further increased to 5.2 M, the well-defined truncated octahedra were appeared, which composed of eight hexagonal {111} facets and six square {100} facets (Fig. 2j ~ Fig. 2k), it is worth that the low-index planes {110} disappeared. By progressively increasing the OH^- ions concentration to 6.8 M, the as-obtained Cu_2O crystals possessed perfect octahedral morphology with sharp corners and well-defined edges, which were composed of eight {111} planes (Fig. 2m ~ Fig. 2n). In addition, corresponding simulated structures for different morphologies were provided in Fig. 2c, Fig. 2f, Fig. 2i, Fig. 2l and Fig. 2o: red for {100} facets, green for {110} facets, and reddish orange for {111} facets. From the above results, cubic, edge-truncated cubic, edge- and corner-truncated octahedral, truncated octahedral and octahedral Cu_2O architectures have been successfully synthesized by a facile hydroxyl-assisted aqueous approach. According to Steno's law, the angles between two corresponding facets on the crystals are constant, so the crystallographic planes can be well-defined.[26,27] Figure. S1 displays the measured interfacial angles of this typical morphology, and the crystallographic planes can be well-defined.

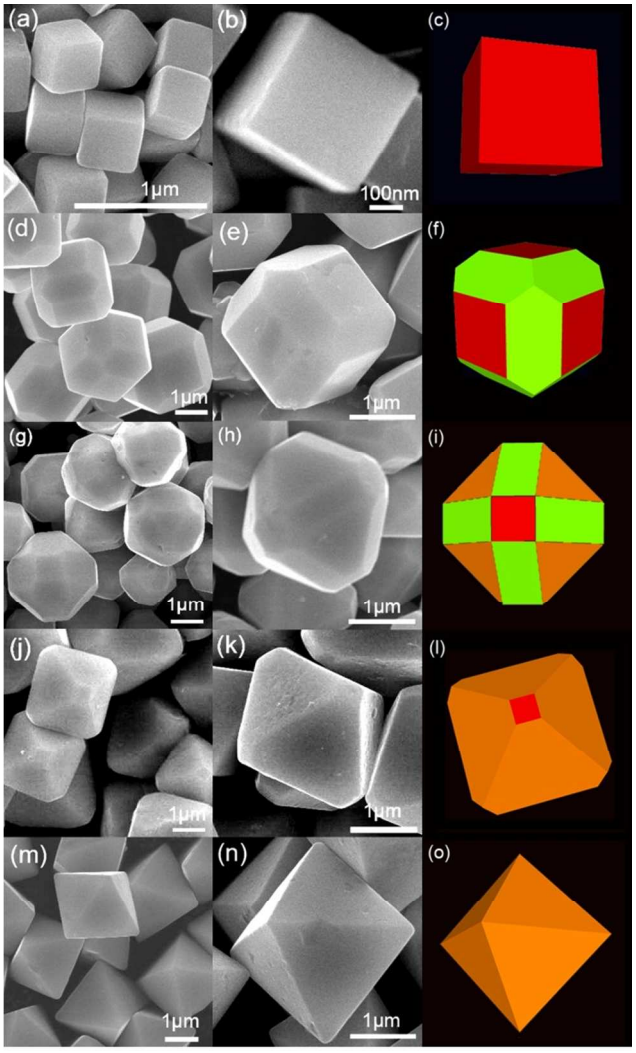

Fig. 2 Typical SEM images of the Cu_2O crystal with various morphologies synthesized by altering the concentration of NaOH. (a-c) cubes, 0.6 M; (d-f) edge-truncated cubes, 1.6 M; (g-i) edge- and corner-truncated octahedra, 3.96 M; (j-l) truncated octahedra, 5.2 M; (m-o) octahedra, 6.8 M. And corresponding simulated structures of Cu_2O crystals were expressed with different colors in Fig. 2f: red for {100} facets, green for {110} facets, and reddish orange for {111} facets.

The controlled experiment without using ligand is conducted under otherwise the same conditions, rhombicuboctahedral Cu_2O crystals have been obtained as shown in Figure. S2, which may be attributed to the quick release rate of the Cu^{2+} due to the absence of the effective coordinated effect of EDTA.[28]

In the Cu_2O crystal lattice, the surface atom structures of {100}、{111} and {110} facets are fully different. {100} facets of Cu_2O are predominated by Cu or O atoms only, leading to the electrically neutral state of {100} facets usually.[29] The {111} and {110} facets are formed with Cu and O atoms and the Cu atoms with dangling bonds which can make them positively charged, but {110} planes has a higher density of "Cu" dangling bonds than that of the {111} planes. A stronger adsorption between negative OH^- ions and the Cu atoms on the {111} and {110} facets than the other {100} facets has been indicated.[30,31] From the above experiments results and crystal growth theory, a possible formation mechanism can be proposed as follows.

When the concentration of OH^- ions was lower, the growth rate along the ⟨111⟩ direction far exceeds that of the ⟨100⟩ direction, the {100} facets were remained because of their lower growth rates, therefore the cubic morphology was formed.[32] As the concentration of OH^- ions was from 0.6 M to 1.6 M, the increase of OH^- ions caused a relatively faster growth rate along the <100> direction, resulting into the shrinking of the <100> direction, meanwhile, {110} facets had a higher density of Cu dangling bonds than {111} facets, so {110} facets had a higher adsorbing capacity with OH^- ions than {111} faces, which leads to a lower growth rates ratio along the <110> than the <111> direction. Thus the edge-truncated cubes with {100} and {111} facets appeared.[31] As the concentration of OH^- ions further increase, the excess OH^- ions would adsorbed on the {111} facets, so the edge- and corner-truncated octahedra with {111} facets were generated.[31]When the concentration of OH^- ions was further increase, the reduction reaction was enhanced which may change the growth rates along the <111> directions and <100> directions, therefore truncated octahedra and octahedra were formed.[32] From the above results, the compositions of the final products were affected by the hydroxyl-dependent reduction reactions.[20]

The shape-dependent photocatalytic activities of the as-prepared polyhedral Cu_2O crystals were investigated on the decomposition of methylene orange (MO) in aqueous solution under visible-light irradiation. The orange color of the MO solution gradually diminished on xenon lamp irradiation in the presence of photocatalysts, indicating the degradation of MO. UV-vis spectra was used to investigate the photocatalytic degradation activity of the MO dye. The characteristic absorption peak of MO at 465 nm was used as a monitoring parameter during the catalytic degradation process (Figure.S3). When irradiated for 4 h, the decomposition of the MO aqueous solution in the presence of the above samples is as follows as showed in Fig. 3: edge- and corner-truncated octahedra (91%) > edge-truncated cubes (82%) > octahedra (58%) > truncated octahedra (49%). After irradiated under visible light for 4 h, the XRD patterns and SEM images of these sample showed a pure phase of Cu_2O crystals (Figure.S4-S5), but edge-truncated cubes and edge- and corner-truncated octahedra showed that the surfaces were not smooth, which illuminated that the etching was slighter.

The underlying photodegradation mechanism might involve the electron–hole pair separation by irradiation and subsequent scavenging of the electrons and trapping of holes by shape-dependent Cu_2O semiconductors, leading to the fabrication of

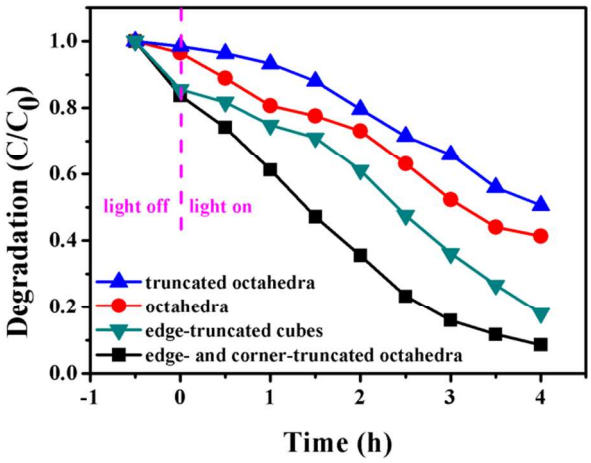

Fig. 3 The curves of photodegradation of MO by Cu_2O edge- and corner-truncated octahedra**,** edge-truncated cubes**,** octahedra and truncated octahedra, respectively.

the active oxidants. As visible light was irradiated, Cu_2O semiconductors would produce electrons and holes.[33] On the account of Cu_2O crystal had a strong adsorption capacity for oxygen molecules, the electrons accumulated on the facets of Cu_2O crystal may be scavenged by adsorptive O_2 to yield O^{2-}, which further reacts with H_2O and electrons to produce hydrogen peroxide (H_2O_2) and the hydroxyl radical ($^{\bullet}OH$) which can effectively bleach the MO (eqn (4-9)). In our experiment, octahedra with entirely {111} facets are much more photocatalytically active than truncated octahedra, which may be due to the presence of the low-active {100} building blocks of truncated octahedra.[32] Compared octahedra and truncated octahedra, edge- and corner-truncated octahedra and edge-truncated cubes have more edges and corners, which could improve photocatalytic activity.[31,34-36] The MO (negative charge) could preferentially adsorb onto the highly active surfaces because of their coordination unsaturated Cu dangling bonds (positive charge) of {110} and {111} facets, therefore photocatalytic activities of {111} and {110} facets are higher than that of {100} facets. On the other hand, edge- and corner-truncated octahedra have higher relative areas of {110} and {111} facets than edge-truncated cubes (Fig. S6-S7), therefore edge- and corner-truncated octahedra had higher photocatalytic activity than that of edge-truncated cubes, which has been demonstrated by the previous report.[31] The results clearly demonstrate that photocatalytic activity is highly dependent on the exposed surface facets.[34]

$$Cu_2O + h\nu \rightarrow e^- (CB_{Cu2O}) + h^+ (VB_{Cu2O}) \quad (4)$$

$$2H_2O \rightarrow O_2 + 4H^+ + 4e^- \quad (5)$$

$$O_2 + e^- \rightarrow O_2^- \quad (6)$$

$$O_2 + 2H_2O + 2e^- \rightarrow H_2O_2 + 2OH^- \quad (7)$$

$$H_2O_2 + O_2^- \rightarrow {}^{\bullet}OH + OH^- + O_2 \quad (8)$$

$$^{\bullet}OH + MO \rightarrow \text{degradation products} \quad (9)$$

In summary, uniform and monodisperse cubic, edge-truncated cubic, edge- and corner-truncated octahedral, truncated octahedral and octahedral Cu_2O architectures were synthesized via a facile solution–phase synthesized route. It is well-established that hydroxyl play an important role in morphology-evolution process. The shape-dependent effect of the Cu_2O microcrystals on photocatalytic degradation of MO has been investigated.

Acknowledgements

This work was supported by National Science Foundation of China (NSFC No. 51302213 and 51272209), Doctoral Fund of Ministry of Education of China (No. 20120201120051), Shaanxi Province Science and Technology Innovation Team Project (2013KCT-05), Youth Foundation of Shaanxi Province of China (No. 2012JQ6007), and Fundamental Research Funds for the Central Universities of China.

Experimental

Materials

$CuSO_4{\cdot}5H_2O$, EDTA, $C_6H_6O_2$ and NaOH were obtained from Aladdin reagent. All chemicals used in our experiment were of analytical grade and used without further purification. Deionized water (18.25 MΩ•cm) from a MilliQ Academic water purification system (Millipore Corp.) was used in all preparations.

Synthesis of morphological Cu_2O architectures

For the syntheses of Cu_2O crystals with various morphologies from cubic to octahedral structures, 2 mmol $CuSO_4.5H_2O$ and 1 mmol EDTA were dissolved in 30 mL deionized water using a breaker, after 30 min, heated to 55°C, then 25 mL of NaOH solution with different concentrations of 0.6 M, 1.6 M, 3.96 M, 5.2 M, 6.8 M were added into the above solution, after being stirred for 5 min later, 0.5 g $C_6H_6O_2$ was added into the solution under a constant stirring at 55°C for 1.0 h to obtain the desire products, and then cooled to room temperature naturally, the samples were centrifuged at 8000 rpm for 1 min (XIANYI TG16-WS centrifuged). The brick red precipitates were collected and washed with deionized water and anhydrous ethanol many times, respectively. Finally they were dried at 60°C for 6 h in a vacuum oven.

Notes and references

School of Science, State Key Laboratory for Mechanical Behavior of Materials, MOE Key Laboratory for Non-Equilibrium Synthesis and Modulation of Condensed Matter, Xi'an Jiaotong University, Xi'an 710049, ShaanXi, People's Republic of China.

E-mail: zmyang@mail.xjtu.edu.cn (Z. M. Yang).

†Electronic Supplementary Information (ESI) available: Additional SEM images, XRD patterns and absorption spectra of MO solution.

1 A. O. Musa, T. Akomolafe and M. J. Carter, *Sol. Energy Mater. Sol. Cells*, 1998, **51**, 305.

2 J. Ramírez-Ortiz, T. Ogura, J. Medina-Valtierra, S. E. Acosta-Ortiz, P. Bosch, J. Antonio de los Reyes and V. H. Lara, *Appl. Surf. Sci.*, 2001, **174**, 177.

3 J. Zhang, J. Liu, Q. Peng, X. Wang and Y. Li, *Chem. Mater.*, 2006, **18**, 867.

4 B. Laik, P. Poizot and J. Tarascon, *J. Electrochem. Soc.*, 2002, **149**, A251.

5 Z. Wang, S. Zhao, S. Zhu, Y. Sun and M. Fang, *CrystEngComm*, 2011, **13**, 2262.

6 Z. Zhang, J. Sui, L. Zhang, M. Wan, Y. Wei and L. Yu, *Adv. Mater.*, 2005, **17**, 2854.

7 W. Z. Wang, G. H. Wang, X. S. Wang, Y. J. Zhan, Y. K. Liu and C. L. Zheng, *Adv. Mater.*, 2002, **14**, 67.

8 J. Zhang, J. Liu, Q. Peng, X. Wang and Y. Li, *Chem. Mater.*, 2006, **18**, 867.

9 W. Zhou, B. Yan, C. Cheng, C. Cong, H. Hu, H. Fan and T. Yu, *CrystEngComm*, 2009, **11**, 2291.

10 S. Sun, D. Deng, C. Kong, Y. Gao, S. Yang, X. Song, B. Ding and Z. Yang, *CrystEngComm*, 2011, **13**, 5993.

11 S. Sun, C. Kong, S. Yang, L. Wang, X. Song, B. Ding and Z. Yang, *CrystEngComm*, 2011, **13**, 2217.

12 H. Y. Zhao, Y. F. Wang and J. H. Zeng, *Cryst. Growth Des.*, 2008, **8**, 3731.

13 S. Sun, F. Zhou, L. Wang, X. Song and Z. Yang, *Cryst. Growth Des.*, 2009, **10**, 541.

14 X. Wang, C. Liu, B. Zheng, Y. Jiang, L. Zhang, Z. Xie and L. Zheng, *J. Mater. Chem. A*, 2013, **1**, 282.

15 X. Liang, L. Gao, S.Yang and J.Sun, *Adv. Mater.*, 2009, **21**, 2068.

16 Q. Hua, D. Shang, W. Zhang, K. Chen, S. Chang, Y. Ma, Z. Jiang, J. Yang and W. Huang, *Langmuir*, 2011, **27(2)**, 665.

17 W. Wang, P. Zhang, L. Peng, W. Xie, G. Zhang, Y. Tu and W. Mai, *CrystEngComm*, 2010, **12**, 700.

18 H. Zhang, Q. Zhu, Y. Zhang, Y. Wang, L. Zhao and B. Yu, *Adv. Funct .Mater.*, 2007, **17**, 2766.

19 H. Zhang, X. Zhang, H. Li, Z. Qu, S. Fan and M. Ji, *Cryst. Growth Des.*, 2007, **7**, 820.

20 K. Chen and D. Xue, *CrystEngComm*, 2012, **14**, 8068.

21 W. Huang, L. Lyu, Y. Yang and M. H. Huang, *J. Am. Chem. Soc.*, 2012, **134**, 1261.

22 Y. Cao, J. Fan, L. Bai, F. Yuan and Y. Chen, *Cryst. Growth Des.*, 2009, **10**, 232.

23 M. Basu, A. K. Sinha, M. Pradhan, S. Sarkar, A. Pal, C. Mondal and T. Pal, *J. Phys. Chem. C*, 2012, **116**, 25741.

24 J. Li, J. Wu, X. Zhang, Y. Liu, D. Zhou, H. Sun, H. Zhang and B. Yang, *J. Phys. Chem. C*, 2011, **115**, 3630.

25 J. Ho and M. H. Huang, *J. Phys. Chem. C*, 2009, **113**, 14159.

26 H. Yang and H. Zeng, *Angew. Chem.*, 2004, **116**, 6056.

27 X. Zhao, Z. Bao, C.Sun and D. Xue, *Cryst. Growth*, 2009, **311**,711.

28 H. Zhang, X. Zhang, H. Li, Z. Qu, S. Fan and M. Ji, *Cryst. Growth Des.*, 2007, **7**, 820.

29 Z. Yang, S. Sun, C. Kong, X. Song and B. Ding, *J. Nanomater.*, 2010, **2010**, 70.

30. D. Zhang, H. Zhang, L. Guo, K. Zheng, X. Han and Z. Zhang, *J.Mater. Chem.*, 2009, **19**, 5220.

31 Y. Zhang, B. Deng, T. Zhang, D. Gao and A. Xu, *J. Phys. Chem. C*, 2010, **114**, 5073.

32 Z. L. Wang, *J. Phys. Chem. B*, 2000, **104**, 1153.

33 S. Sun, X. Song, Y. Sun, D. Deng and Z. Yang, *Catal. Sci. Technol.*, 2012, **2**, 925.

34. M. H.Huang, S. Rej and S. Hsu, *Chem. Commun.*, 2014, **50**, 1634.

35 R. Narayanan and M. A. El-Sayed, *J. Phys. Chem. B*, 2005, **109**, 12663.

36 Y. Xiong, H. Cai, B. J. Wiley, J. Wang, M. J. Kim and Y. Xia, *J. Am. Chem. Soc.*, 2007, **129**, 3665.

